Turkish Journal of Physics

Volume 26 | Number 6 Article 9

1-1-2002

Defect Structure of Glow Peak 1 in LiF:Mg,Ti (TLD-100)

A. NECMEDDİN YAZICI

Follow this and additional works at: https://journals.tubitak.gov.tr/physics

 Part of the Physics Commons

Recommended Citation

YAZICI, A. NECMEDDİN (2002) "Defect Structure of Glow Peak 1 in LiF:Mg,Ti (TLD-100)," *Turkish Journal of Physics*: Vol. 26: No. 6, Article 9. Available at: https://journals.tubitak.gov.tr/physics/vol26/iss6/9

This Article is brought to you for free and open access by TÜBİTAK Academic Journals. It has been accepted for inclusion in Turkish Journal of Physics by an authorized editor of TÜBİTAK Academic Journals. For more information, please contact academic.publications@tubitak.gov.tr.

Turk J Phys
26 (2002) , 473 – 481.
© TÜBİTAK

Defect Structure of Glow Peak 1 in LiF:Mg,Ti (TLD-100)

A. Necmeddin YAZICI
University of Gaziantep, Department of Engineering Physics,
27310, Gaziantep-TURKEY
e-mail: yazici@alpha.bim.gantep.edu.tr

Received 28.01.2002

Abstract

The possible defect structure of peak 1 of LiF:Mg,Ti (TLD-100) was studied in the present work after different pre-irradiation heat treatments between 80°C and 150°C using the computer glow curve deconvolution (CGCD) method. It was shown that the defect structure of peak 1 is based on colloid centers, Ti^{+4}-$3O_2^-$-mixed centers and U_1-centers.

Key Words: Thermoluminescence, LiF:Mg,Ti, TLD-100, defect structure, U-centers.

1. Introduction

Lithium Fluoride has ionic crystal structure and, when doped with Magnesium and Titanium ($Li^{+1}F^{-1}$: Mg^{+2},Ti^{+4}) becomes a phosphorescence material that is now widely used in the thermoluminescence dosimetry of ionizing radiations. Owing to its application in personnel dosimetry, thermoluminescence (TL) studies on LiF:Mg,Ti have received wide attention [1] and many investigations have been made to understand the basic TL mechanism of this material during the past 45 years [2]. A large number of papers have been published to describe its basic TL mechanism and dosimetry properties, among which are [1-10]. In spite of the extensive works devoted to the identification of the lattice defects responsible for the different TL peaks in LiF:Mg,Ti, its TL mechanism is still not well understood [10-12]. Despite improvements in recent years, there are still many contradictions in the structure of the defects [13-14]. It is well known that, if the defect structure of in LiF:Mg,Ti were better known, then the TL mechanism will be better understood. Therefore, many experimental methods, such as optical absorption, dielectric loss, ionic conductivity, electron spin resonance and TL emission, have been employed to understand the nature of defects in this material along with-or without-pre- and post-thermal annealing treatments [2]. Thus data obtained by these methods has resulted in the development of many models, of which two have become particularly well-known. One model interprets the dipoles formed by Mg^{+2}-cation vacancies as acting trapping centers [15], while the other model is based on Z-centers formed by pairs of Mg^{+2}-electron occupied anion vacancies [16].

In general, there are two kinds of glow peaks in the glow curve of TL materials, i.e. long- and short-lived peaks. For example, if the glow curve of LiF:Mg,Ti is measured immediately after irradiation, it exhibits a multi-peak structure with low and high temperature peaks between room temperature and 250°C and all of the individual glow peaks are numbered starting from peak 1 to 5. Peak 1 is a short-lived peak in the glow curve of LiF:Mg,Ti. Despite the many disagreements about its decay time in the literature, it is largely expected that decay time is approximately 30 min following irradiation. Therefore, it is required to state that this peak is useless in dosimetric investigations due to the its short-life. Moreover, it is well known there are high relationships between the responsible defects and peaks in LiF:Mg,Ti. For example, it has

been suggested that peak 2 and 3 were directly related to Mg^{+2} dipoles and peak 4 and 5 were related to the higher-order clusters of Mg^{+2}dipoles according to the first model [15]. However, the structure of defect of peak 1 was not considered in all published materials up to now. But, we think that if the structure of defect responsible with this peak can be better understood then it could suggest better defect models to the other glow peaks between 2 and 5 due to the high relationships between them. In the present work, we inrestigated to understand the possible structure of defect of peak 1 using TL and phototransfer thermoluminescence (PTTL) methods after suitable heat treatments.

2. Methods

Thermoluminescence method is a relatively complex process since it involves both a trap and a luminescence center. When an insulator or semiconductor is exposed to ionizing radiation at room or at low temperature, electrons are released from the valance band to the conduction band. This leaves a hole in the valance band. Both types of carriers become mobile in their respective bands until they recombine or until they are trapped in lattice imperfections in the crystalline solids. These lattice imperfections play a very crucial role in the TL process. The trapped electrons may remain for a long period when the crystals are stored at room temperature. They can be released due to the sufficient energy given to the electron when the crystal is heated. These electrons may move in the crystalline solid until they recombine with suitable recombination centers that contain holes resulting in the emission of TL light, the spectrum of which is called the TL glow curve. This process of light emission by thermal stimulation from a crystalline solid after irradiation is called as "thermally stimulated process", or simply "thermoluminescence". The nature of crystal defects has been investigated over the past 60 years. In principle, TL measurements provide a very sensitive indication of complex defects in insulators and some semiconductors. But the study of defect structures (model) in solids using only this method is perhaps the most difficult. In fact, this technique has only limited value in arriving at a true characterization of the defect structure of the solid under study. Therefore, this type of measurement has been supplemented by many other experimental techniques.

After incomplete annealing of an irradiated TL sample, the residual trapped charge carriers remain in the deep traps. In the phototransfer process, during the illumination of the sample with ultraviolet light, the residual electrons from the deep traps can be transferred into empty shallow trapping sites and this process can induce regeneration of the filled shallow traps. Then the filled shallow traps give regenerated lower-temperature glow peaks during second heating cycle. The phenomenon is called phototransfer thermoluminescence. The deep traps in the phototransfer process act as donors and the shallow traps as acceptors.

Often illumination with ultraviolet light induces low-temperature glow peaks, but it is also seen to diminish high-temperature glow peaks (residual deep traps). This can be interpreted as the release of charge from the deep traps. This increase in lower temperature glow peaks, at the expense of a decrease in the high-temperature glow peaks, shows the appearance of a transfer of charge between centers. Therefore, the phototransfer thermoluminescence technique can be used in order to understand the electronic charge nature of defect centers in the crystalline solid. If the lower-temperature glow peak is regenerated and the size of the high-temperature peak is decreased, they can be thought of as having electron type defect centers otherwise they can be considered as hole centers.

3. Experimental Procedures

In this study, LiF:Mg,Ti single crystalline chips which were obtained from Harshaw-Bicron Chemical Company with dimensions 3.2 x 3.3 x 0.89 mm^3. Samples were heat-treated using a microprocessor controlled electrical oven operated at different temperatures for different intervals ranging between 1 min to 72 hours. The temperature was measured and continuously monitored during the annealing period with a thermocouple that was placed in close proximity to the samples. The temperature sensitivity of the oven was estimated to be $\pm 1^{\circ}$C for the whole temperature range at which the samples were heat-treated. All samples were first annealed at 410 $\pm 1^{\circ}$C for 30 min followed by fast quenching to room temperature (approximately 500°C/min) and then re-annealed for selected times at a desired temperature before irradiation. After annealing, the samples were exposed to β-rays from a ^{90}Sr-^{90}Y-source. The irradiation equipment is an additional part of

the 9010 Optical Dating System and is interfaced to a PC computer via a serial RS-232 port. The time duration between irradiation and TL readout was always kept constant at about 45 sec. Glow curve readout was carried out on a platinum planchet at a linear heating rate of $2^{\circ}Cs^{-1}$ up to 400°C using a Harshaw QS 3500 Manual type TL reader which is interfaced to a personnel computer, where all recorded glow curves were analyzed. In this way, each glow curve can be analyzed using a best-fit computer program that was developed at the IRI, Delft, The Netherlands [17], based on a Marquardt algorithm minimization procedure. The program resolves the individual peak present in the curve, giving the best values for the different peak parameters. Two different models were used in the computer program. In the first model, the glow curve is approximated from the first order TL kinetics by the expression

$$I = n_0 s \exp(-\frac{E_a}{kT}) \exp[-\frac{s}{\beta}\frac{kT^2}{E_a} \exp(-\frac{E_a}{kT})(0.9920 - 1.620\frac{kT}{E_a})], \quad (1)$$

whereas in the second model the glow curve is approximated with the general order TL kinetics by using the expression

$$I = n_0 s \exp(-\frac{E_a}{kT})[1 + \frac{(b-1)s}{\beta}\frac{kT^2}{E_a} \exp(-\frac{E_a}{kT})(0.9920 - 1.620\frac{kT}{E_a})]^{\frac{b}{1-b}}, \quad (2)$$

where n_0 (m^{-3}) is the number of trapped electrons at t=0 sec, s (sec^{-1}) is the frequency factor, E_a (eV) is the activation energy, T (K) is the absolute temperature, k (eV/K) is Boltzmann's constant, β (K/sec) is the heating rate and b is the kinetic order.

For PTTL measurements, the irradiated samples were first annealed at 180°C for 10 sec in the TLD reader to remove glow peaks 1−5 and then cooled to room temperature. The samples were, then, put kept in a liquid nitrogen vacuum cryostat which was placed into a Aminco-Bowman-2 luminescence-spectrometer. The spectrometer applied a monochromatic UV illumination using its 150 W high pressure Xe lamp and grating monochromator. PTTL glow curves were measured at a heating rate of 20 K/min.

4. Results

A typical glow curve of a TLD-100 sample, which received only standard heat treatment (410 ±1°C for 30 min) and then beta irradiated for 2 Gy, is shown in Figure 1. Each peak number is illustrated on the glow curve. For a 2°C/s heating rate, the peak temperatures are obtained at ≈65°C (peak 1), 118°C (peak 2), 160°C (peak 3), 190°C (peak 4), 220°C (peak 5), and 287°C (peak 7).

The composite set of glow curves readout with same heating rate (2°C/sec), annealed for selected times at various temperatures, is shown in Figures 2a-d. The height of each peak varies from batch to batch of the crystals when also the same heating rate was used. Therefore, in this study, four crystal chips were used at each annealing temperature, but their average was taken into consideration.

From Figures 2a and 2b, it is clearly seen that at low pre-annealing temperatures (≤100°C), the intensity of peak 1 is first quickly decreased with increasing annealing time. It is also clearly seen from these glow curves that the other low temperature glow peaks 2 and 3 also decreased with increasing annealing time. The separation of peak 4 from peak 5 is very difficult due to the merging of peak 4 into 5 following annealing, at low temperatures (≤100°C). Figures 2c and 2d show sets of the glow curves aged for different times at intermediate temperatures 125°C and 150°C, respectively. At these temperatures for long annealing times, some new glow peaks grow between peak 3 and 4, and peak 5 and 7. Therefore, the resolution of glow curves for long annealing times at high annealing temperatures becomes very difficult.

The normalized peak area of some glow peaks, as a function of pre-irradiation annealing time at 80, 100, 125 and 150°C, are shown in Figure 3a-d, respectively. The trends observed for the peak areas are as follows:

The peak areas of the low temperature glow peaks (1−3) first decrease, then start to increase with increasing annealing times at low annealing temperatures below 100°C. The intensity of peak 5 slightly increases and then decreases, whereas peak 4 considerably increases and then decreases at low pre-irradiation annealing temperatures. However, at 125 and 150°C, the intensity of peaks 4 and 5 immediately decrease

with annealing times, except a slightly initial growth up to 15 min at 125°C. However, the trends of low temperature glow peak areas are very different from each other at high pre-irradiation annealing temperatures. At 125°C, after a slight decrease, the intensity of peak 1 continuously increases up to performed time. On the other hand, the intensity of peak 2 continuously decreases with increasing annealing time. Peak 3 represents a similar trend with peak 1, except that after approximately 5 hours it becomes approximately constant. At 150°C, the intensity of peak 1 immediately starts to increase and reaches a saturation point where it is approximately four times greater than the intensity without any annealing treatment. On the other hand, the intensity of peaks 2 and 3 sharply decreases with increasing annealing times; and peak 3 is completely converted to another type of peak, namely peak 3a [18], after approximately 30 minutes. However, the decay time of peaks 2 and 3 at 150°C take place more rapidly than at 125°C. From Figure 3, it can be understood that peak 1 has different defect structure character than other peaks yet they are completely related to each other.

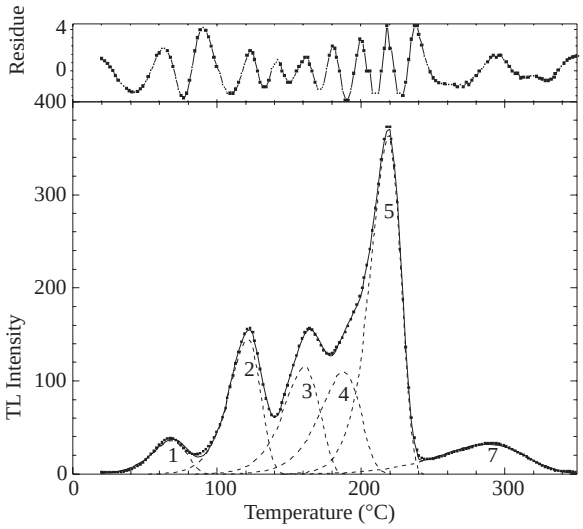

Figure 1. An analyzed glow curve of TLD-100 after an annealing at 400°C for 1 h followed by rapid cooling (β=2°Cs^{-1}). In the figure, dots denote experimental points, continuous lines show global fitting and the fitted peaks are represented by broken lines.

Figure 4 shows the PTTL glow curve of LiF:Mg,Ti samples which were illuminated by monochromatic UV lights at 195 nm at liquid nitrogen temperature for 30 min. As shown in this figure, peak 1 is clearly present in the PTTL glow curve but its peak temperature is approximately 10°C lower than recorded glow curves in TL measurements. This difference is due to the heating rate difference between the TL and PTTL measurements. In this study, we have also applied different wavelength to the samples and we have observed that, after each illumination, PTTL glow curves are similar to each other but with small differences in the intensity of glow peaks. From the results of PTTL glow curves, one can easily draw the conclusion that peak 1 completely arises from electron-type traps.

5. Discussion and Conclusions

In determining the nature, of the trapping centers in TL materials, there are two main problems. One is the atomic nature of the trap; and the other is its electronic charge nature whether it is an electron or hole type of trap. The PTTL is a very useful technique to understand the electronic charge nature of defect centers in the TL materials. It is the best candidate to show that the regenerated glow peaks in PTTL glow curves are due to the electron type of traps. In this study, we have observed that peak 1 is always regenerated after UV illumination at all applied wavelengths in PTTL measurements. So, peak 1 has a completely electron type of trap because of its regeneration after PTTL measurements.

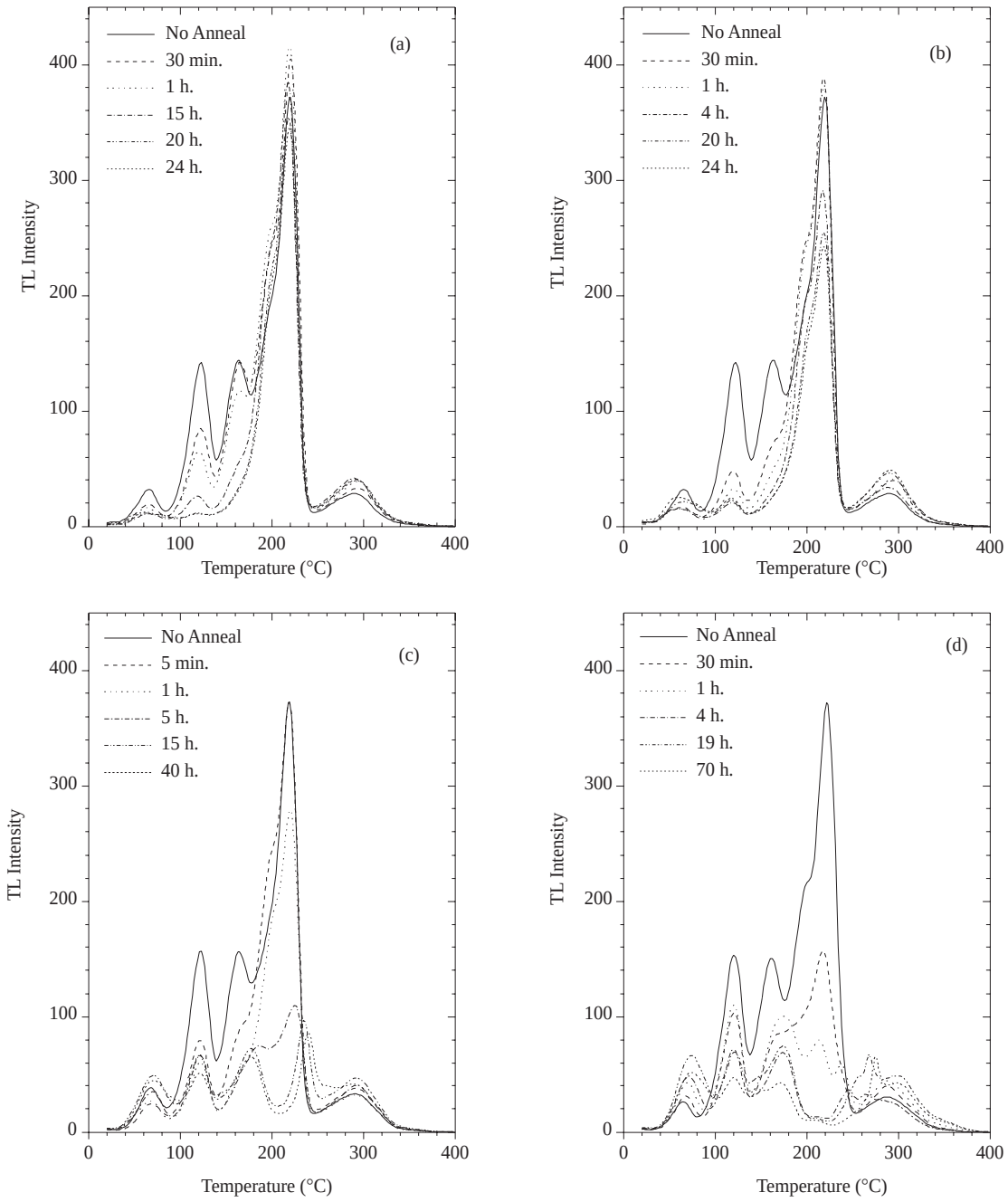

Figure 2. A set of thermoluminescence glow curves for TLD-100 samples after pre-irradiation heat treatments at (a) 80°C; (b) 100°C; (c) 125°C; (d) 150°C for different annealing times ($\beta = 2^{\circ}\mathrm{Cs}^{-1}$ and dose level 2 Gy).

In the literature, many experimental techniques have been employed to understand the atomic nature of the trapping centers in TL materials [2]. However, interpretation of the obtained data using these methods has not proved to be straightforward due to the extreme complexity of the data for LiF:Mg,Ti. In recent years, a new defect model, which is based of the specially correlation of Mg/Ti-related defects, has been widely used to explain the relation between glow peaks and their corresponding defects [6]. According to this new model, TL peak 5 arises from Mg-trimer/Ti-related defect complexes.

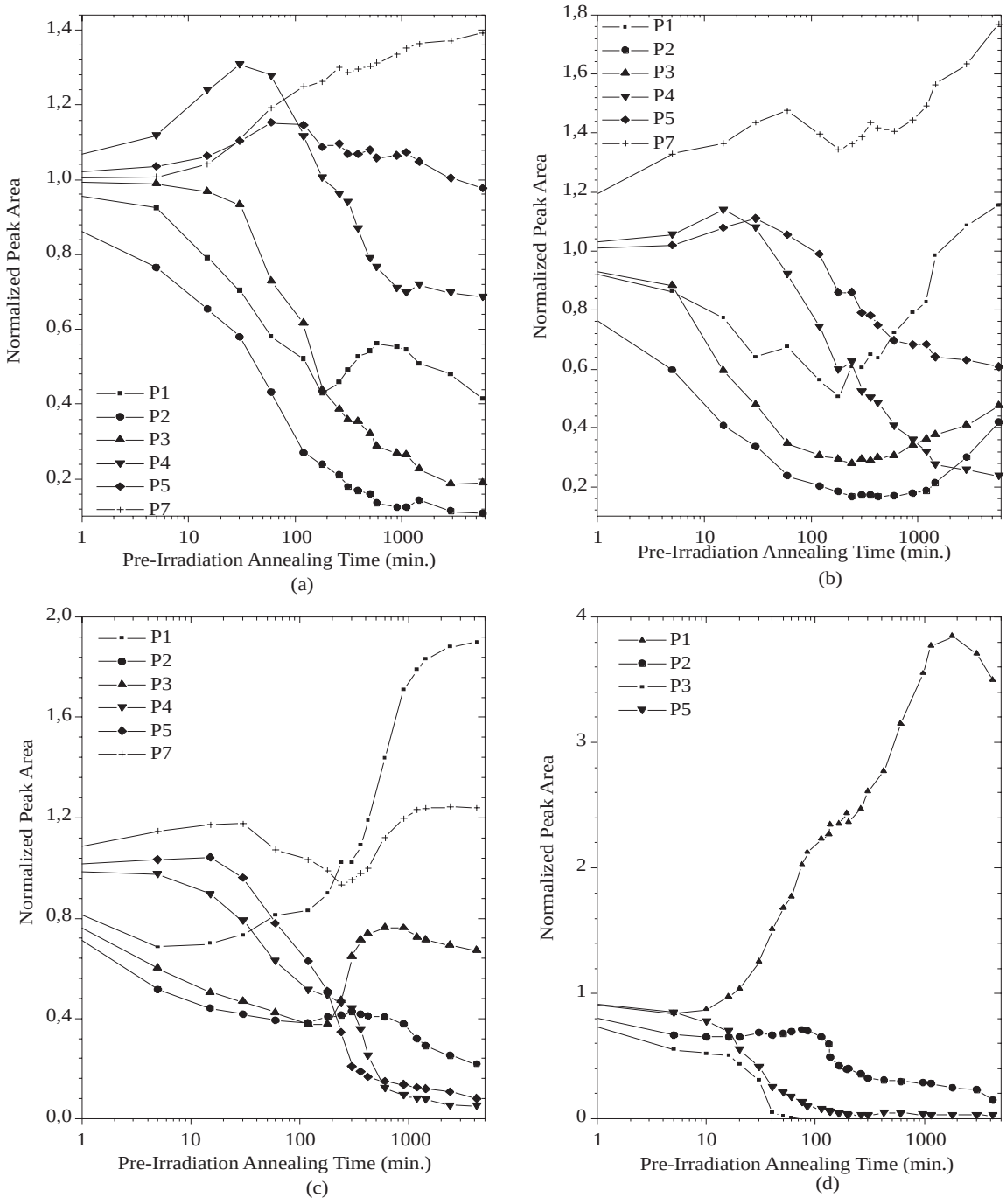

Figure 3. Normalized peak areas versus log of annealing at (a) 80°C; (b) 100°C; (c) 125°C; (d) 150°C for all glow peaks registered from glow curves at a linear heating rate of $2^{\circ}Cs^{-1}$.

The role and structure of hydroxyl (OH)-ions in the alkali halide crystals have been studied over the forty years and it was shown that these ions play critical roles both in TL trapping and recombination (luminescence) process [2]. Recent investigations have shown that LiF:Mg,Ti contains a high concentration of OH-ions as background impurities and they have nearly the same mass and atomic radii as Fluorine (F^-) ions and therefore easily diffuse into the LiF lattice during crystal growth or by annealing the samples in air at elevated temperatures [19−20]. These experimental investigations have also shown that TL glow curve

shapes and sensitivity of LiF:Mg,Ti are highly dependent on the concentration of OH-ions, because, both Ti and Mg-ions are highly desirous in that they easily form defect complexes with OH-ions. On the other hand, OH-ions firstly prefer to combine with available Ti-ions and, after the saturation of all Ti-ions, the additional OH-ions would form complexes with Mg-ions. Therefore, the TL sensitivity of this material increases with increasing the concentration of OH-ions up to saturation of all Ti ions by OH-ions and then starts to decrease at higher OH-levels [21]. Experimental investigations on the OH-doped alkali halide crystals have shown that OH-ions decompose into substitutional oxygen ions, hydrogen ions and F centers during irradiation [22]. In spite of the unclear situation of Ti-ions in the LiF lattice, it has been accepted that Ti-ions usually enter into the lattice substitutionally for Li^{+} in Ti^{4+} state owing to the absence of ESR signals. However, the ESR spectra of Ti containing LiF samples are yet not fully understood due to its very complex superposition. Moreover, Ti^{3+}-related defects were detected by EPR after irradiation but disappeared again during the thermoluminescence readout [23]. Using ESR and EPR signals, Davies considered that the possible defect structure model could be Ti^{4+}-ions bound to three OH^{-} ions at or near neighbor positions as Ti^{4+}-$3OH^{-}$ before irradiation and as $Ti^{3+}F_3^{-}$ O_3^{-} after irradiation [23]. On the other hand, He et al. have concluded that the possible charge states of Ti-ions depend on the experimental parameters (i.e. annealing) before irradiation and therefore Ti^{2+}-ions were also observed by them using optical absorption experiments after heat treatment [24].

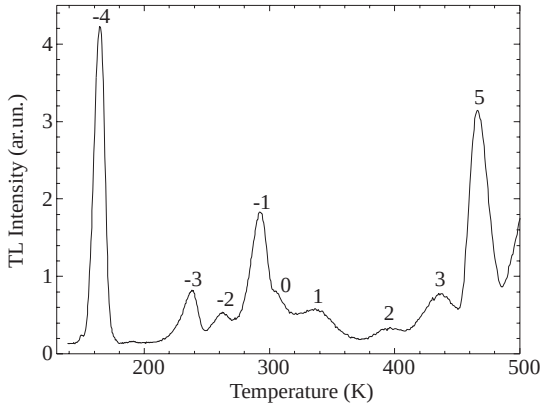

Figure 4. The PTTL glow curve of LiF:Mg,Ti between 120 and 500 Kelvin.

The first decrease in the intensity of peak 1 at low annealing temperatures can be attributed to Ti^{4+}-OH^{-} defect complexes that associate with Mg^{+2}-cation vacancies (Mg-dipoles) and produce Ti^{4+}-OH^{-}/Mg-trimer defect complexes which are responsible for high temperature peaks 4 and 5. Therefore, these peaks immediately start to increase owing to the increase of Ti^{4+}-OH^{-}/Mg-trimer defect complex (LC/TC) at low annealing temperatures below 100°C. However, for further annealing times, these peaks start to decrease due to the beginning formations of higher order clusters of Mg-related defects, also showing an increase in low temperature peaks. This situation can be explained that precipitate phases (colloid centers) start to form with increasing annealing time. During the formation of colloid centers, firstly OH-ions and then Ti-ions start to dissociate from these centers. At intermediate annealing temperature, 125°C, low temperature peaks 1, 2 and 3 immediately start to decrease and then, after approximately ten minutes, the intensity of peak 1 increase slightly for up to 5 hr. For further annealing times, its intensity shows a sharp increase up to 20 hours and then the increase continues with a decreasing slope. High temperature peaks 4 and 5 show similar decay trends and following a slightly initial growth up to 15 min, the intensities continuously decrease with increasing annealing time at low annealing temperatures. This situation can be explained as that the association of Ti and Mg-related defects become faster at high annealing temperatures than at low annealing temperatures and therefore low temperature peaks decrease while peak 5 increases. But, after approximately 15 minutes, the formation of precipitate phase starts and therefore OH- and Ti-ions start to dissociate from colloid centers. Therefore, peak 1 starts to increase whereas peaks 4 and 5 to decrease.

At around 150°C, the decay periods of high temperature peaks 4 and 5 immediately start and occur very rapidly and, therefore, it can be stated that at this temperature (150°C) the variations in defect structures

are more effective than the other temperatures. So, the formation of the precipitate phase immediately starts and continues with increasing annealing time. Then, OH and Ti-ions are quickly dissociated from colloid centers from which peak 1 immediately starts to increase. From these explanations, it is well understood that the intensity of peak 1 is always directly related to the concentrations of colloid centers, OH-ions, Mg and Ti-related defects. For example, the Ti and Mg-impurity related defects associate to form Ti^{4+}-OH^{-}/Mg-trimer (LC/TC) defect complexes for short annealing times at low annealing temperatures (i.e. below 100°C) and therefore the intensity of peak 1 is quickly decreased. But, its intensity again started to increase at the beginning of formation of colloid centers for long annealing times. Additionally, the concentration of colloid centers immediately started to increase at high annealing temperatures and thereupon the intensity of peak 1 immediately started to increase. The separated OH and Ti-ions from colloid centers settled down in the place of Fluorine (F^{-}) and Lithium (Li^{+})-ions just near the colloid centers, respectively. The OH-ions decompose into three parts [O_2^{-}, U-based centers (U_1, U_2, U_3), and F-centers] after irradiation. The oxygen ions remain in the anion sites previously occupied by OH-ions and yielding Ti-ion complexes containing oxygen ions and/or cation vacancies. The hydrogen atom can be found in the alkali halides in three different forms. The U band is due to the substitutional H^{-}-ions, the U_1 belongs to interstitial H^{-}-ions, and the U_2 center is due to atomic hydrogen in an interstitional position H^0. The trapped entities of peak 1 should be related with H-ions and Ti-related defects that are produced after irradiation. Because, the hydrogen related U-based centers are no longer stable at room temperature as peak 1 and they quickly decay with recombination with nearby Ti-related defects that are located at the near sites of colloid centers, yielding TL emission that can be described by the relation

$$U_1 - \text{ centers } + Ti^{+4} - 3O_2^{-} - \text{ mixed centers } \xrightarrow{\text{TL Process}} \{Ti^{+3} - 3O_2^{-}\}^{*} + U_2$$

$$\xrightarrow{\text{TL Process}} Ti^{+3} - 3(OH^{-}) + h\nu$$

The U-based and Ti-related defects after irradiation should be electron and hole traps, respectively. The U-based centers are reasonably interstitional H^{-} ions (U_1-centers), and during the TL process these ions, indirectly, (by first emitting their electrons) or directly recombine with Ti-related defects that is probably Ti^{4+}-$3O_2^{-}$ mixed centers instead of $Ti^{3+}F_3^{-}$ or $Ti^{3+}F_3^{-}$ O_3^{-} centers which were proposed by Davies using EPR measurements [23].

As a result, we point out in the present paper that the intensity of peak 1 in TLD-100 is directly related with the concentrations of colloid centers, OH-ions, Mg and Ti-related defects. The U_1 and Ti^{4+}-$3O_2^{-}$ mixed centers might be the electron and hole trapping defect structures of peak 1, respectively.

References

[1] Y.S. Horowitz, Thermoluminescence and Thermoluminescence Dosimetry, V1-3, CRC Press, Inc. Boca Raton, Florida, (1984).

[2] S.W.S. McKeever, M. Moscovitch and P.D. Townsend, Thermoluminescence Dosimetry Materials : Properties and Uses, Nuclear Technology Publishing, (1995).

[3] R.M. Grant and J.R. Cameron, *J. Appl. Phys.*, **37**, (1966), 3791.

[4] G.C. Taylor and E. Lilley, *J. Phys. D: Appl. Phys.*, **15**, (1982), 1253.

[5] F. Sagastibelza and J.L. Alvarez Rivas, *J. Phys. C: Solid State Phys.*, **14** (1981) 1873.

[6] S.W.S. McKeever, *J. Appl. Phys.*, **68(2)**, (1990), 724.

[7] R. Chen and S.W.S. McKeever, Theory of Thermoluminescence and Related Phenomena, World Scientific, Singapore, (1997).

[8] R. Chen and Y. Kirsh, Analysis of Thermally Stimulated Pocesses, Pergamon Press, Oxford, (1981).

[9] S.W.S. McKeever, Thermoluminescence of Solids, Cambridge University Press, Cambridge, (1985).

[10] G. Kitis and T. Otto, *Nucl. Instr. and Meth. B*, **160**, (2000), 262.

[11] A.N. Yazici, *Radiat. Prot. Dosim.*, **80**, (1998), 379.

[12] S.W.S. McKeever and Y.S. Horowitz, *Radiat. Phys. Chem.*, **36**, (1990), 35.

[13] Y. Weizman, Y.S. Horowitz, and L. Oster, *J. Phys. D: Appl. Phys.* **32**, (1999), 2118.

[14] Y. Weizman, Y.S. Horowitz, L. Oster, D. Yossian, O. Bar-Lavy, and A. Horowitz, *Radiat. Meas.*, **29(5)**, (1998), 517.

[15] X.L. Yuan and S.W.S. McKeever, *Phys. Stat. Sol. (a)*, **108**, (1988), 545.

[16] A.N. Yazıcı and Z. Öztürk, *Phys. Stat. Sol. (b)*, **209**, (1998), 195.

[17] A.J.J. Bos, T.M. Piters, J.M. Gomez Ros, and A. Delgado, GLOCANIN, IRI-CIEMAT Report 131-93-005 IRI Delft, 1993.

[18] A.N. Yazıcı and Z. Öztürk, Phys. Stat. Sol. (a), Accepted for Publications.

[19] T.G. Stobe and L.A. DeWerd, *J. Appl. Phys.*, **57(6)**, (1985), 2217.

[20] H. Vora, J.H. Jones and T.G. Stobe, *J. Appl. Phys.*, **46(1)**, (1975), 71.

[21] W. Wachter, N.J. Vana, and H. Aiginger, *Nucl. Instr. and Meth.*, **175**, (1980), 21.

[22] J.H. Schulman and W.D. Compton, Color Centers in Solids, Pergamon Press, (1962).

[23] J.J. Davies, *J. Phys. C: Solid State Phys.*, **7**, (1974), 599.

[24] S.S. He, J.F. Merklin, Q. Sun and Q. Wang, *Phys. Stat. Sol. (a)*, **145**, (1994), K1.